On the capability of unsteady RANS to predict transonic buffet

Sebastian Illi* Thorsten Lutz* Ewald Krämer*

22.06.2012

Abstract

On common transport aircraft, unsteady and complex shock boundary layer interaction called shock buffet, occurs at transonic Mach numbers and high lift coefficients. Due to shock induced separations at the suction side of the wing, a self sustained shock movement is established, which may lead to fluctuations in the load of the wing. These fluctuations, if of large enough amplitude, can pose a serious risk to the integrity of the structure of the wing.

For industrial CFD applications, eddy viscosity models became very popular in the last decade and are used for different problems in subsonic and transonic flow, but their accuracy to predict buffet onset seems to be uncertain. Simulations on an OAT15A airfoil using different meshes have been performed where the influence of the mesh topology shows different behaviour from convergence to steady state solutions to shock movement over the whole airfoil.

Due to these results a more sophisticated approach was used to simulate shock buffet on an airfoil. A Reynolds stress model based on an epsilon equation in homogenous form, which was implemented in TAU during the first funding period of FOR 1066 has been applied to the problem. It is shown that this model provides reliable behaviour on all types of meshes and shows good representation of the buffet phenomena even in the regime of buffet onset.

Nomenclature

b	span [m]
c	chord length [m]
c_L	lift coefficient [-]
c_p	pressure coefficient [-]
f	frequency [Hz]
M	Mach number [-]
Re	Reynolds number [-]
α	angle of attack [°]
δ_{TE}	trailing edge thickness [m]

*Institute of Aerodynamics and Gas Dynamics, University of Stuttgart, Pfaffenwaldring 21, 70569 Stuttgart

1 Introduction

One of the goals of the German research project ComFliTe (Computational Flight Testing), involving the German Aerospace Centre (DLR), EADS and several universities, is to extend the simulation capabilities of CFD to the boundaries of the flight envelope to estimate the loads beyond regular flight conditions. At the Institute of Aerodynamics and Gas Dynamics (IAG) at the University of Stuttgart the flight regime in the area of transonic shock buffet has been investigated. Here complex shock boundary layer interaction leads to an excitation of the integral force and moment coefficients which can pose a serious risk to common aircraft.

Before the three-dimensional simulations on an aircraft will be obtained, a more academic case on an airfoil in transonic buffet conditions was investigated using unsteady RANS (URANS) methods. Therefore the experimental data base by Jacquin et al. about self sustained shock movement on an OAT15A airfoil [4] was used. The aerodynamics on an airfoil in transonic buffet conditions is characterized by strong shock boundary layer interaction which leads to a separation near the foot of the shock. The separation bubble grows and reduces the effective camber of the airfoil. Therefore the shock is shifted upstream where the pre-shock Mach number is reduced and the shock loses strength. The shock boundary layer interaction is weakened and the flow reattaches followed by a shock motion downstream where the shock gains strength again. The feedback loop is closed and the cycle continues.

Tijdeman [18] showed that this shock movement is associated with disturbances generated around the trailing edge and called them *Kutta-Waves* named after the Kutta condition at the trailing edge. Lee described these waves outside the detached flow region as an energy transfer mechanism to maintain the oscillatory shock movement [9]. He also determined the time to travel for sonic waves from the shock to the trailing edge and back to the shock as the time period for the shock motion. Fig. 1 shows a sketch of these waves as it can be found in [8].

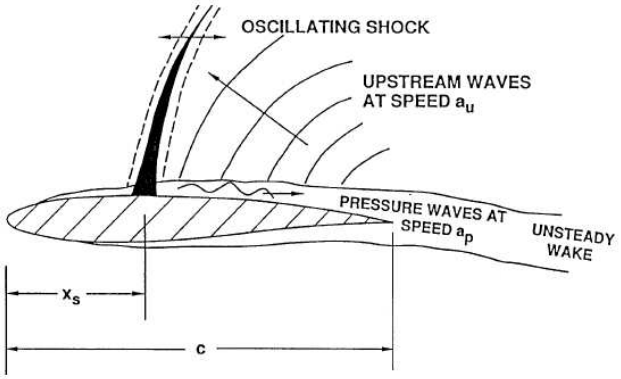

Figure 1: Model of self-sustained shock oscillation (from Ref. [8])

Alshabu et al. confirmed the existence of pressure waves originating from the trailing edge of a BAC3-11 airfoil in a wind tunnel [1]. They further revealed these waves to be regarded as weak shocks, which may also influence the transition of the boundary layer.

Jacquin et al. published wind tunnel data of an OAT15A airfoil in transonic buffet conditions [4]. Related to these measurements Deck published numerical results of this test case [3]. He performed CFD simulations with the ONERA elsA code using URANS techniques and his own developed ZDES approach. He showed that in the region of buffet onset the URANS approach using a Spalart-Allmaras one-equation model is not able to capture the unsteady shock

movement at $\alpha = 3.5°$ while his zonal approach was able to represent the buffet phenomenon. The comparison of the spectra showed encouraging results due to the good representation of the shock movement frequency and the higher harmonics. On the way downstream of the shock movement position he described an enrichment of the spectrum at the higher frequencies. Deck accounts the rollup eddies of the free shear layer impacting the thick trailing to be responsible for this part of the spectrum. He further described that this interaction is responsible for upstream moving pressure waves, which regenerate again an instability leading to a feedback mechanism described by Lee [9]

2 Numerical Method

2.1 The DLR TAU Code

The following CFD simulations have been performed with the unstructured finite volume solver TAU [11]. The code is developed by the German Aerospace Center (DLR) and used by several German universities and the aircraft industry. Explicit time stepping using a multistep Runge-Kutta scheme is available as well as an implicit Backward-Euler time stepping scheme. Flux discretization is implemented using various upwind or a central scheme with scalar and matrix artificial dissipation. The code achieves very good parallel performance on modern high performance computers and contains several convergence accelerators like local time-stepping, geometrical multigrid or residual smoothing. Unsteady simulations are available due to dual and global time stepping schemes.

2.2 Turbulence Models

2.2.1 Eddy viscosity models

In TAU different turbulence models have been implemented. The eddy viscosity models make use of the Boussinesq assumption which uses a linear relationship between the Reynolds stresses and the velocity gradients. The linear factor between these quantities is called the turbulent viscosity which is directly modelled by the one-equation models.

For the following investigations namely the Spalart-Allmaras model (SAO) and its modification the Strain Adaptive Spalart Allmaras model (SALSA) has been used. These turbulence models are often used in CFD due to their simplicity and robust behaviour. Only an additional transport equation for $\tilde{\nu}$, a derivative of the turbulent viscosity, is solved [17]. The SALSA approach extends the capability of the SAO model to predict non-equilibrium conditions. Changes to the original model are made in the definition of the production and diffusion term and the shear stress tensor. A detailed description of the model can be found in [15].

As a representative of the two-equation models the popular Shear Stress Transport model (SST) is used. Here a transport equation for the turbulent kinetic energy k and the turbulent dissipation rate ω is solved. It uses a blending function to switch between k-ω and k-ε like behaviour and is extended with a limiter function for the turbulent viscosity ν_t. The model can be found in detail in [10].

Furthermore the Linearized Explicit Algebraic k-ω turbulence model (LEA) [16] is investigated. It is based on the Wilcox k-ω model but uses a different definition for the eddy viscosity. It is known to have good shock prediction capabilities in transonic flows.

2.2.2 ε^h Reynolds stress model

The Reynolds stress models solve a set of additional transport equations derived from the Navier-Stokes equations to model the components of the Reynolds stress tensor directly. Here, the recently developed and implemented ε^h-RSM turbulence model according to [5] and [14] has been applied using the Reynolds stress modelling equation

$$\frac{Du_iu_j}{Dt} = P_{ij} + \Phi_{ij} - \epsilon_{ij} + D^{\nu}_{ij} + D^{t}_{ij} \tag{1}$$

with the production term P_{ij} and the viscous diffusion D^{ν}_{ij}. Based on DNS results near-wall damping functions have been calibrated to model the pressure-strain correlation Φ_{ij}. The homogenous part ϵ^h_{ij} of the dissipation rate $\epsilon = \epsilon^h + \frac{1}{2}D^{\nu}$ is accounted with

$$\frac{D\epsilon^h}{D_t} = -C_{\epsilon 1}\frac{\epsilon^h}{k}\overline{u_iu_j}\frac{\partial U_i}{\partial x_i} - C_{\epsilon 2}f_{\epsilon}\frac{\epsilon^h\tilde{\epsilon}^h}{k} + C_{\epsilon 3}\nu\frac{k}{\epsilon^h}\overline{u_ju_k}\frac{\partial^2 U_i}{\partial x_j\partial x_l}\frac{\partial^2 U_i}{\partial x_k\partial x_l} + D_{\epsilon^h} + S_l + S_{\epsilon 4}. \tag{2}$$

Finally the anisotropic dissipation rate tensor ϵ^h_{ij} follows

$$\epsilon^h_{ij} = f_s\overline{u_iu_j}\frac{\epsilon^h}{k} + (1-f_s)\frac{2}{3}\delta_{ij}\epsilon^h. \tag{3}$$

3 Description of the test case

Investigations have been performed for the ONERA test case on the OAT15A airfoil in transonic buffet onset conditions. Measurement data exists from the transonic S3Ch wind tunnel of Onera-Meudon Center in France [4]. The model has a chord length of $c = 230$mm with a span of $b = 780$mm and a thick trailing edge of $\delta_{TE}/\mathrm{c} = 0.5\%$. Measurements have been performed at a Mach number domain ranging from $M = 0.70$ to $0.75 \pm \cdot 10^{-4}$ at angles of attack ranging from $\alpha = 2.4°$ to $3.91°$ to determine the area of transonic buffet onset. The Reynolds number Re equals 3 million based on the chord length c and the stagnation temperature T is quantified to be around 300K. Boundary layer transition was tripped at a fixed position $x/c = 7\%$ on the suction and pressure side of the airfoil.

The OAT15A model was equipped with 68 static pressure sensors and additionally 36 Kulite™ sensors to measure the unsteady pressure fluctuations. Additionally schlieren films have been recorded at a frequency of 1000Hz and Laser Doppler Velocimetry (LDV) data of the phased averaged longitudinal velocity component $\langle u \rangle$ and its RMS values $\langle u'u' \rangle$ have been published.

For the URANS simulations in the following sections the case with a Mach number $M = 0.73$ at a angle of attack $\alpha = 3.9°$ was investigated. This case is expected to be beyond the buffet onset conditions and a clear shock motion is seen in the averaged pressure distribution and its RMS values. The shock movement frequency for these conditions was determined to be around 69Hz and clearly seen with its higher harmonics in the pressure spectra.

4 Results obtained with eddy viscosity models

4.1 Influence of grid resolution

To investigate the influence of the turbulence model in transonic buffet conditions a parametric study on three block structured meshes and a hybrid mesh has been performed. The block structured meshes are of C-type topology and vary in number of cells by a factor of two. Therefore the cell spacing has been factorized by a factor of 1.4 in the x- and z-direction. Because the simulations have been only performed on two-dimensional meshes the y- direction is neglected in this factorization. The x-axis points into the chord direction, the y-axis along the spanwise extend and the z-axis complements to a right hand coordinate system.

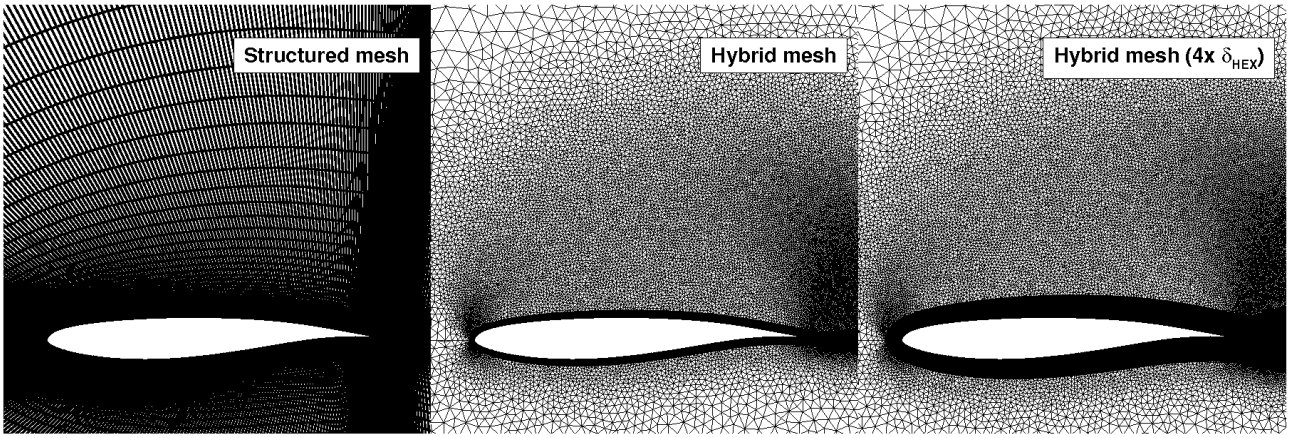

Figure 2: Grid topologies for the URANS simulations

Additionally a hybrid mesh based on the boundary layer cells of the structured coarse mesh and a surrounding unstructured block has been generated. The height of the hexahedral area is estimated via the analytic result for the boundary layer thickness of a flat plate multiplied by a safety factor of two. Around this area prisms are used to fill the space between the rectangular cells and the farfield boundary. Above the suction side of the airfoil the prism block has been refined to better resolve the area around the shock.

Figure 3 shows the result for central differences discretization with scalar dissipation based on the formulation of Jameson [7]. The different colours symbolize the turbulence models. The different shape of the symbols represents the different meshes used for the simulation.

For the SST model only a small shock movement leading to a small c_L-amplitude is seen on the coarse structured and the hybrid mesh. On the structured meshes, as for the SAO and the LEA model on all meshes, the solutions converge to steady state and are therefore not shown in Fig. 3. This result is comparable to the URANS results of Deck [3], where also no shock buffet was seen below $\alpha = 4.5°$ using the ONERA elsA code.

Only the SALSA model is capable of representing the shock buffet phenomenon on all meshes. Here buffet occurs with a frequency around 75Hz which is in acceptable agreement with the experimental data of Jacquin [4]. Admittedly the amplitude of the lift coefficient is massively underestimated. A higher resolution of the structured mesh improves the result a little but the amplitude c'_L is still around half the value of the measurement. A switch to the hybrid mesh leads to a similar result with an increased frequency around 82Hz.

Due to the consistent values obtained with the SALSA model, a deeper look on the results is done. In Fig. 4(a) the averaged pressure coefficient c_p resulting from the SALSA simulation on

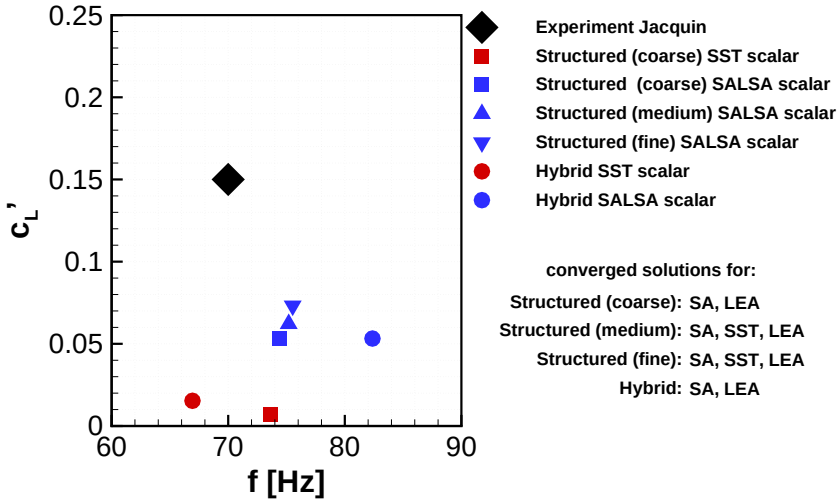

Figure 3: Frequency and amplitude of the shock movement for different turbulence models on various meshes with scalar dissipation

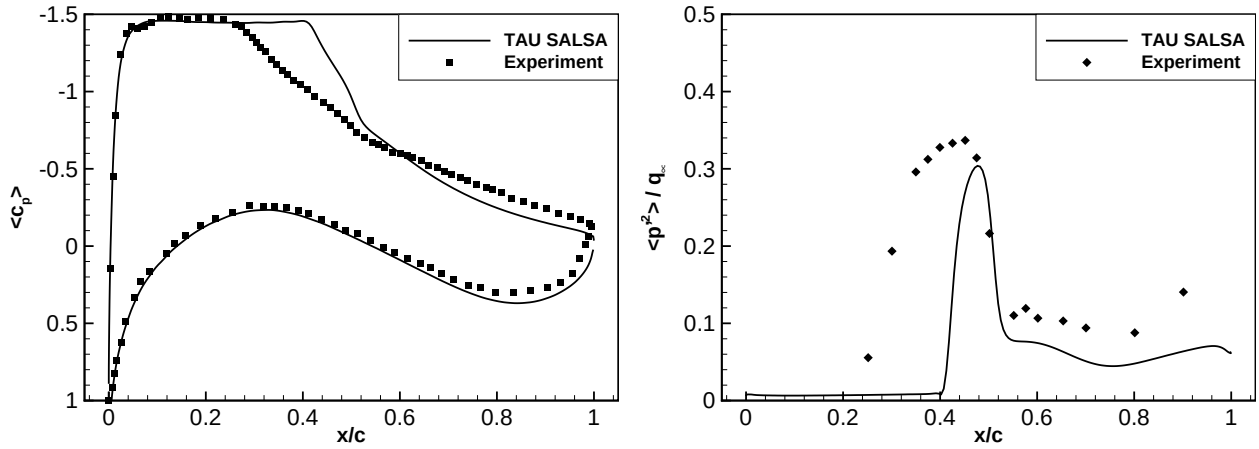

(a) c_p-mean distribution

(b) c_p-RMS distribution on the suction side

Figure 4: Results for the SALSA model on the medium structured mesh with scalar dissipation

the structured medium grid is compared to the experimental distribution. One can find good agreement on the pressure side of the airfoil. Also on the suction side the c_{p-min} is predicted correctly but the shock movement is limited to a regime between $x/c = 0.4$ to 0.5 and therefore the gradient of the mean pressure distribution is only flattened is this area, while the experiment shows an influence of the shock motion up to $x/c = 0.25$. The same result is seen on the right hand side in Fig. 4(b) where the RMS values of the pressure distribution are plotted. Due to the heavy change in pressure as a result of the moving shock on the suction side of the airfoil, a high peak is seen in the RMS values between $x/c = 0.25$ to 0.5. Also the area downstream of the shock motion zone shows increased RMS values due to the unsteadiness of the separated flow in this area. However, the SALSA model returns a too weak shock motion resulting in a slightly underestimated level of RMS pressure values on the suction side of the OAT15A airfoil in a too narrow area. The values in the area of the periodic emerging separation are underpredicted.

In a second study the dissipation scheme of the central fluxes was changed to matrix dissipation [6] with a reduced 4th order coefficient. Fig. 5 shows that the change of the scheme has no major impact on the results on the structured grids. Most of the solutions converge to steady state on these meshes and the SALSA model returns shock buffet in a regime close to the scalar dissipation results. However, the SALSA result on the hybrid mesh is influenced by the transition to the matrix dissipation scheme. The shock movement amplitude is still underpredicted by the model but the overestimated frequency of 82Hz for the scalar dissipation is reduced to a frequency close to the experimental obtained one.

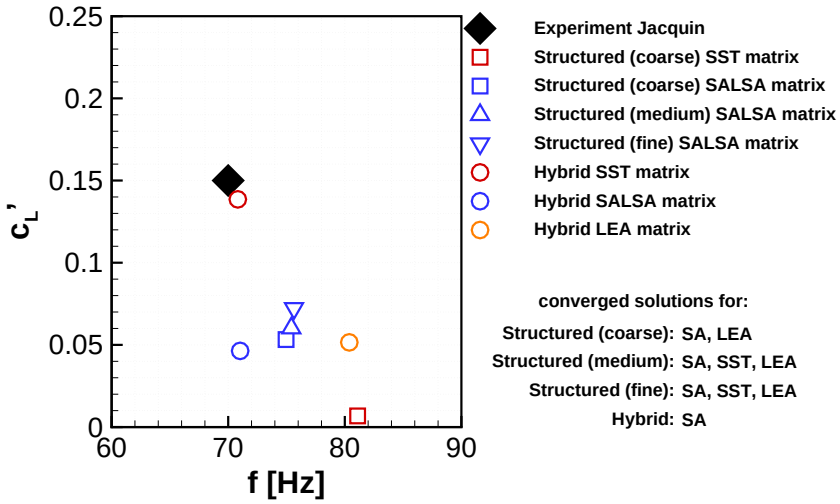

Figure 5: Frequency and amplitude of the shock movement for different turbulence models on various meshes with matrix dissipation

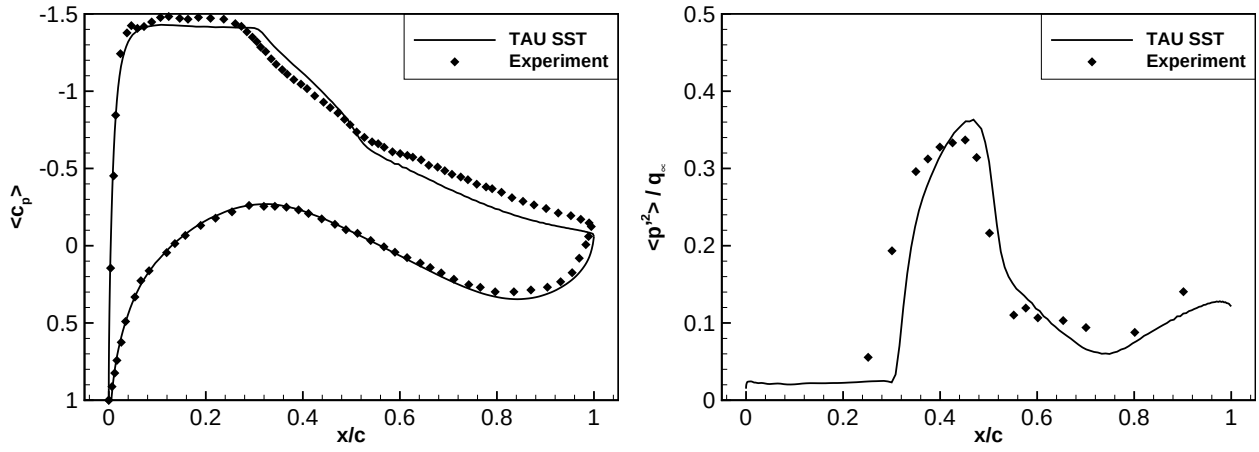

(a) c_p-mean distribution

(b) c_p-RMS distribution on the suction side

Figure 6: Results for the SST model on the hybrid mesh with matrix dissipation

The LEA model, which converged to steady state shows also a little shock movement on the unstructured mesh. But the frequency is overestimated and the c_L-amplitude is way below the measurement result.

A major difference in the results is seen for the SST solution on the unstructured grid where the shock movement with the matrix dissipation scheme now is heavily excited. While in Fig. 3 nearly no change in c_L is seen, the shock motion here leads to a strong change in the integral coefficients and correlates very good with the measured values. Also the frequency is predicted correctly.

Fig. 6(a) shows the mean pressure distribution obtained for the SST turbulence model on the hybrid mesh with matrix dissipation. Very good agreement is obtained on the suction side as well as on the pressure side of the airfoil. Also the RMS values of the pressure distribution are reproduced correctly in respect to magnitude and the shock location area as shown in Fig 6(b). Even in the separate area behind the shock the RMS levels are of the same order of magnitude like in experiment. Although these results look quite promising the fact that on the other meshes the SST model converged to steady state makes doubt about the reliability of the results.

4.2 Influence of hexahedral block height on the SST model results

The strong influence of the mesh topology for the SST model shall be discussed due to the heavy change of the results presented in section 4.1. Hence, the only difference between the structured coarse mesh and the unstructured mesh is the cell type outside of the boundary layer such a strong influence was not expected.

For a parametric study the height of the hexahedral block δ_{HEX} is extended from the unstructured grid by a factor of 2, 4 and 8 to ensure a smooth transition from the hybrid mesh topology to the block structured one. Towards better understanding on the right hand side of Fig. 2 the mesh with the quadrupled hexahedral layer height compared to the normal height δ_{HEX} is plotted.

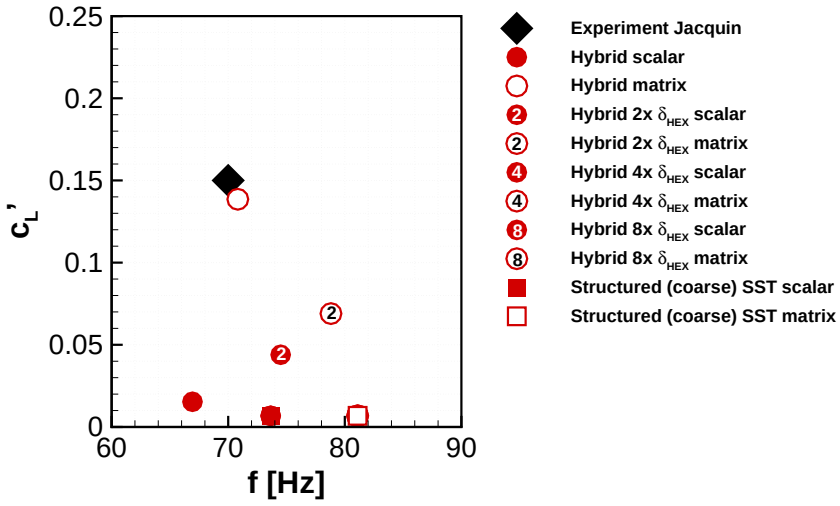

Figure 7: Frequency and amplitude of the shock movement for the SST with changing δ_{HEX}

Fig. 7 shows the results for the different hexahedral block heights δ_{HEX} compared to the results on the coarse structured mesh. Although the result on the hybrid mesh with the standard δ_{HEX} looked quite promising, clear transition to the results of the full structured mesh can be seen for increasing δ_{HEX}. With doubled δ_{HEX} transonic shock buffet is still reproduced by the SST model but the result is much worse than on the standard hybrid mesh. Quadrupled and

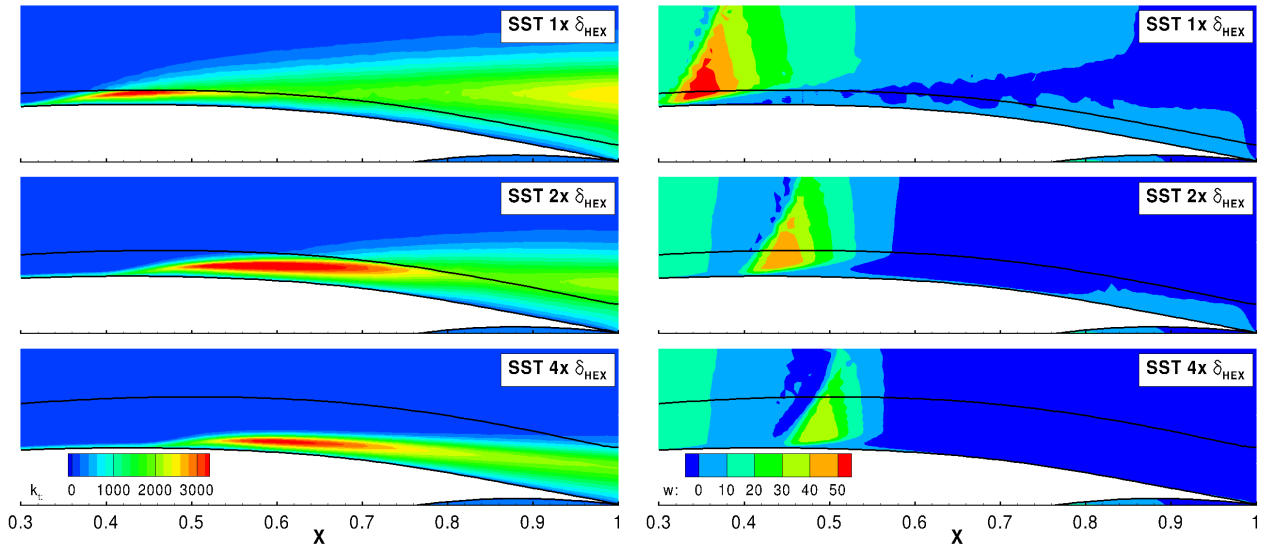

(a) turbulent kinetic energy k_t

(b) z-velocity w

Figure 8: Influence of the hexahedral block height for the SST turbulence model. The most upstream shock position for each mesh is shown.

octupled block δ_{HEX} lead to the same result like on the block structured mesh and therefore converge to steady state.

In search of this behaviour the distribution of the turbulent kinetic energy k_t and the z-velocity component was analysed. Figs. 8(a) and 8(b) show the most upstream position of the shock during a buffet cycle for varying δ_{HEX}. In case of single block height δ_{HEX}, which represents the standard hybrid mesh, the k_t distribution shows a clear discontinuity in wall normal direction so that the hybrid boundary is seen in the solution itself. Due to the large cell growth in the unstructured area and the related diffusive effects, the turbulent kinetic energy is spread in an area far away from the wall. This leads to a strong overestimation of the separation bubble which is followed by a stronger diversion of the mean flow which can be seen in the z-velocity component in Fig. 8(b). The shock is caused to move upstream by this effect and its most upstream location is around the experimental one for the single block height simulation. Although this result seems to look promising in a first place, the effect of the k_t-*burst* seems to be responsible for this kind of *numerical buffet*.

With doubled hexahedral block height only the downstream part of the separation bubble is located in the unstructured part of the mesh. The *numerical buffet* is still present but the shock movement amplitude is decreased significantly. Firstly in the 4x-δ_{HEX}-mesh the whole separation area is located in the structured part but from here on the SST-model is not capable of predicting the shock movement for the chosen case.

Hence, the result depends mainly from the hexahedral block height δ_{HEX}. It is therefore recommended to choose the hexahedral block height at least 10% of the chord length. Also the area ratio of structured and unstructured cells should be around one to obtain a reasonable result with the JST scheme.

5 Results obtained with the ε^h RSM

Besides the eddy viscosity models, the ε^h Reynolds stress model was investigated, which is based on [5] and was further developed and implemented into the TAU by TU Braunschweig and the German Aerospace Centre DLR. Probst et al. already used the model for subsonic problems on a high lift device and obtained reasonable results [13, 12] and Cecora et al. calibrated it for transonic flows [2].

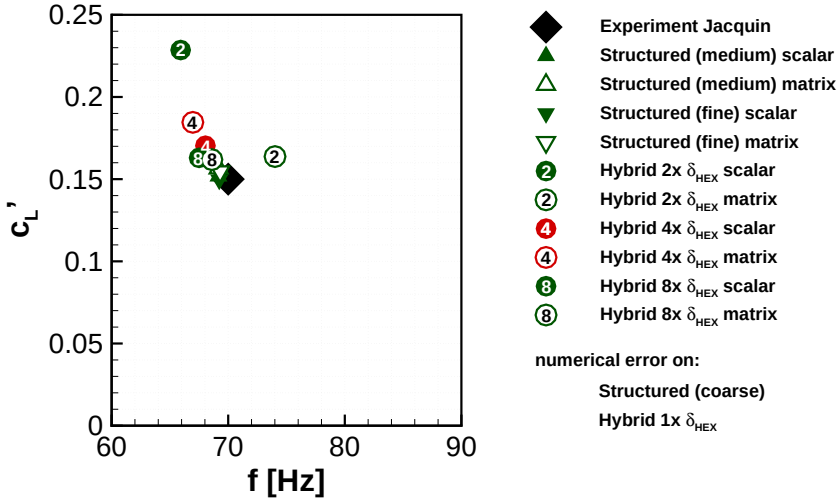

Figure 9: Frequency and amplitude of the shock movement for the ϵ^h RSM on various meshes

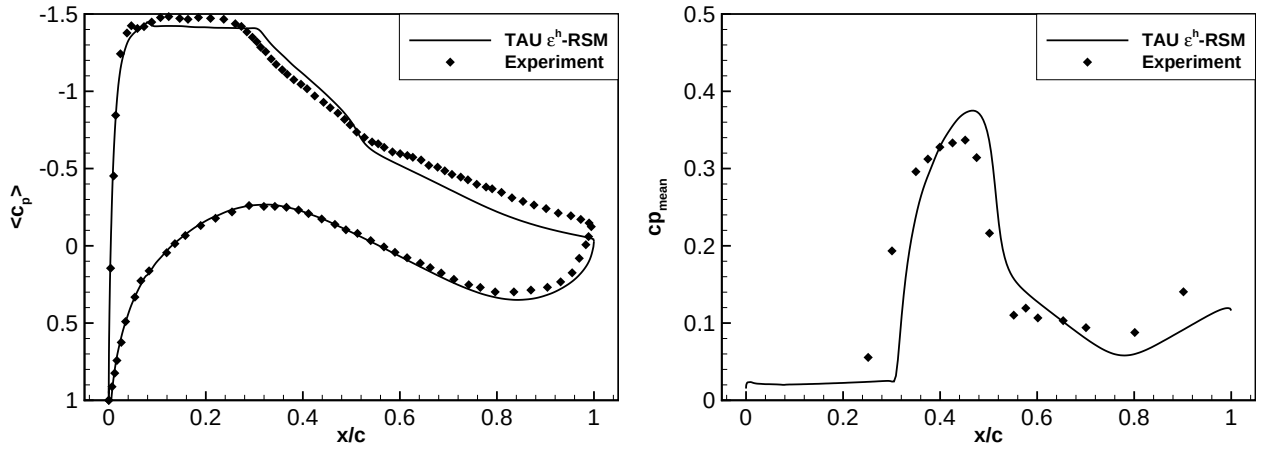

(a) c_p-mean distribution

(b) c_p-RMS distribution on the suction side

Figure 10: Results for the ϵ^h RSM on the coarse hybrid mesh

The model requires a definition of the transition location and a so-called intermittency location to initialize the model with recommended values. For the OAT15A airfoil the transition position of the experiment at $x/c = 7\%$ was used. The intermittency position is located 2% chord in the upstream direction.

The results of the model on the different grids using both the scalar and matrix dissipation scheme is depicted in Fig. 9. The results on the structured meshes are located close to the

experiment data and an increase in resolution improves the result further. Here also the higher quality demands of the RSM are seen, because the coarse mesh leads to an instability followed by numerical error.

The same is seen for the hybrid mesh with standard hexahedral block height, which seems insufficient for the representation of the separation bubble. However, an extend of δ_{HEX} leads to a convergence towards the structured mesh and therefore the experiment values.

A comparison of the mean pressure distribution of the medium mesh and the experiment is shown in Fig. 10(a). The temporal averaged values show excellent agreement with the experiment. The area of shock motion between $x/c = 0.25$ to 0.5 with the reduced pressure gradient is represented by the model. The shock motion can also be seen in Fig. 10(b) where the high RMS levels indicate a strong variance in the pressure distribution. Although the turbulence is not resolved directly by the URANS approach, the RMS values in the separated area behind the shock are well represented.

The mean pressure distribution and the RMS values for the Reynolds Stress model look quite comparable to the SST results in Fig. 6(a) and 6(b), but one has to recognize that the SST result was not consistent on all meshes and the buffet shown there was due to the described k_t-*burst*. Therefore it seems like only the RSM approach is capable to predict the buffet onset correctly while one- or two-equation models show first buffet onset at significant higher angles of attack.

6 Conclusions

In Fig. 11 the magnitude of the density gradient is plotted, which is also known as numerical schlieren to visualize the transonic buffet phenomenon for the RSM. Compared to the eddy viscosity models the separation starting at the foot of the shock (b) is predicted significantly larger and because of the good agreement with the experimental results more realistic. This leads to a stronger reduction of the resulting camber of the airfoil which is followed by a larger movement of the shock location (c)-(e). Reaching its most upstream position the shock becomes weaker and the separation bubble vanishes (f). The shock is able to move downstream again (a) where the shock gains strength and the oscillatory motion continues. Due to their known robustness the eddy viscosity models underpredict the size of the separation bubble or converge to a solution converged to steady state. Therefore they are not capable of predicting the right amplitude and frequency in the shock buffet onset regime. The RSM instead seems to be well calibrated for transonic conditions and correctly determines the size of the separation zone as the effect of reattachment in the most upstream position. These abilities result in a good agreement of frequency and amplitude of the shock motion.

Another major difference in the solution of the RSM can also be found in Fig. 11. After the occurrence of shock induced separation (b) a disturbance moving downstream from the shock to the trailing edge is seen (c). Its interaction with the wake leads to pressure waves starting from the trailing edge (d) and moving upstream outside of the boundary layer (e). In none of the eddy viscosity models these waves were found. This phenomenon was also mentioned by Deck where he described 'upstream-propagating pressure waves' which 'are generated by the impingement of large-scale structures on the upper surface of the airfoil.' [3] As mentioned before Lee describes these waves as a main feature for transonic buffet [9] and calls them necessary as a energy transport mechanism to maintain the self sustained motion. The presence of these waves in the results of the Reynolds stress model might enforce its capability to represent the shock motion leading to a better and more physical result.

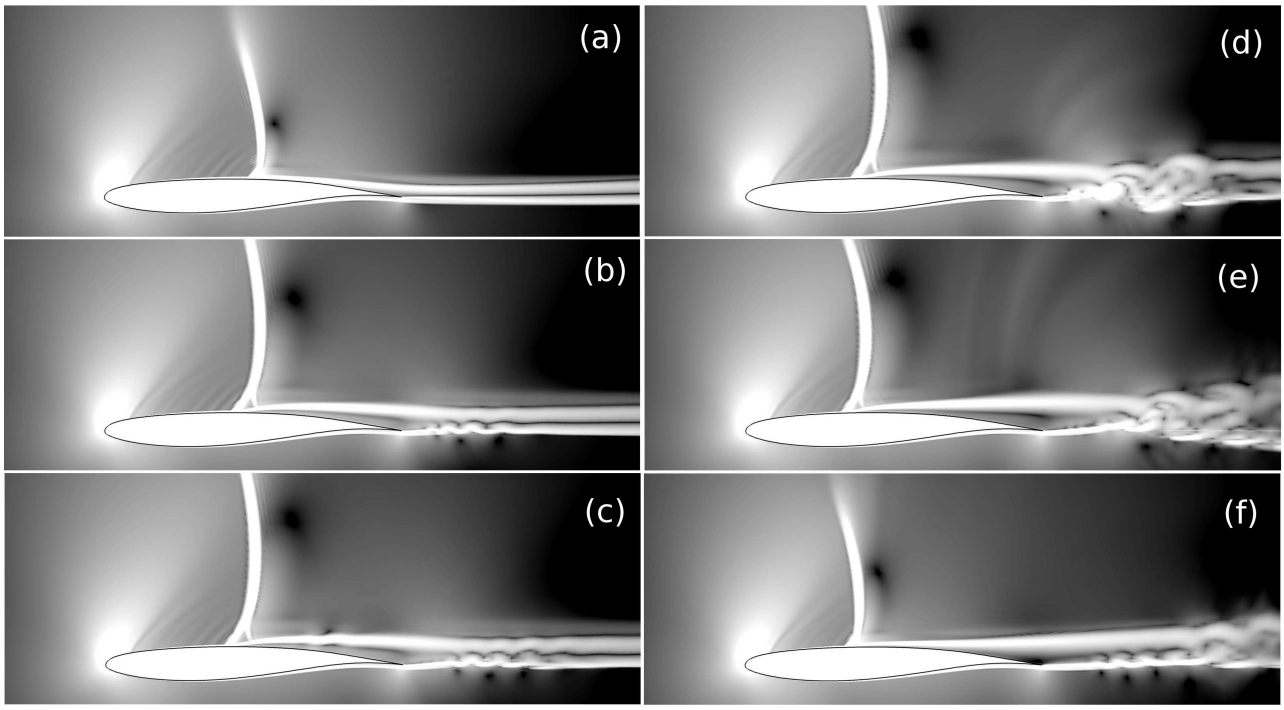

Figure 11: Shock buffet cycle visualization using numerical schlieren with TAU ϵ^h RSM

Acknowledgments

The presented studies are part of the LuFo project "ComFliTe". Our research group gratefully acknowledges the support of the "German Federal Ministry of Economics and Technology" which funded this research.

The computational resources for the simulations were kindly provided by the "High Performance Computing Center Stuttgart".

References

[1] Atef Alshabu, Herbert Olivier, and Igor Klioutchnikov. Investigation of upstream moving pressure waves on a supercritical airfoil. *Aerospace Science and Technology*, 10:465–473, 2006.

[2] R.-D. Cécora, A. Probst, and R. Radespiel. Advanced Reynolds stress turbulence modeling of subsonic and transonic flows. In *Second Symposium Simulation of Wing and Nacelle Stall*, 2010.

[3] S. Deck. Numerical Simulation of Transonic Buffet over a Supercritical Airfoil. *AIAA*, 43:1556–1566, 2005.

[4] L. Jacquin, P. Molton, S. Deck, B. Maury, and D. Soulevant. An Experimental Study of Shock Oscillation over a Transonic Supercritical Profile. In *35th AIAA Fluid Dynamics Conference and Exhibit*, 2005.

[5] S. Jakirlic and K. Hanjalic. A new approach to modelling near-wall turbulence energy and stress dissipation. *Journal of Fluid Mechanics*, 459:139–166, 2002.

[6] A. Jameson, T. J. Baker, and N. P. Weatherill. Calculation of Inviscid Transonic Flow over a Complete Aircraft. *AIAA Paper*, 1986.

[7] A. Jameson, W. Schmidt, and E. Turkel. Numerical Solutions of the Euler Equations by Finite Volume Methods Using Runge-Kutta Time-Stepping Schemes. *AIAA Paper*, 81-1259, 1981.

[8] B. H. K. Lee. Oscillatory shock motion caused by transonic shock boundary-layer interaction. *AIAA Journal*, 28:942–944, 1990.

[9] B. H. K. Lee. Self-sustained shock oscillations on airfoils at transonic speeds. *Progress in Aerospace Sciences*, 37:147–196, 2001.

[10] F. R. Menter. Two-equation eddy-viscosity turbulence models for engineering applications. *AIAA Journal*, 32:1598–1605, 1994.

[11] Institute of Aerodynmaics and Flow Technology. Technical Documentation of the DLR TAU-Code. Technical report, German Aerospace Center (DLR), 2010.

[12] A. Probst, Radespiel R., and Knopp. T. Detached-Eddy Simulation of Aerodynamic Flows Using a Reynolds-Stress Background Model and Algebraic RANS/LES Sensors. In *20th AIAA Computational Fluid Dynamics Conference*, June 2011.

[13] A. Probst, R. Radespiel, and U. Rist. Transition Modelling for Aerodynamic Flow Simulationes with a Near-Wall Reynolds-Stress Model. *AIAA-Journal*, 2011.

[14] A. Probst, R. Radespiel, Ch. Wolf, T. Knopp, and D. Schwamborn. A Comparison of Detached-Eddy Simulation and Reynolds-Stress Modelling Applied to the Flow over a Backward-Facing Step and an Airfoil at Stall. In *48th AIAA Aerospace Sciences Meeting Including the New Horizons Forum and Aerospace Exposition*, 2010.

[15] T. Rung, U. Bunge, M. Schatz, and F. Thiele. Restatement of the Spalart-Allmaras Eddy-Viscosity Model in Strain-Adaptive Formulation. *AIAA Journal*, 41:1396–1399, 2003.

[16] T. Rung, H. Lübcke, M. Franke, L. Xue, F. Thiele, and S. Fu. Assessment of explicit algebraic stress models in transonic flows. In *Proceedings of Fourth International Symposium on Engineering Turbulence Modelling and Experiments*, pages 659–668, Amsterdam, 1999. Elsevier.

[17] P. R. Spalart and S. R. Allmaras. A One-Equation Turbulence Model for Aerodynamic Flows. *AIAA*, 439, 1992.

[18] H. Tijdeman. *Investigations of the transonic flow around oscillating airfoils*. PhD thesis, TU Delft, 1977.